Practical Acceleration Strategies for the Predictive Visualization of Fading Phenomena

Bradley W. Kimmel
University of Waterloo
Waterloo, Ontario, Canada
bwkimmel@cs.uwaterloo.ca

Gladimir V.G. Baranoski
University of Waterloo
Waterloo, Ontario, Canada
gvgbaran@cs.uwaterloo.ca

ABSTRACT

Appearance changes caused by light exposure provide important cues that impart a sense of realism to a computer-generated scene. For instance, a carpet may fade or wood may turn yellow over time as a result of many years of light exposure. In this paper, we analyse the key performance and accuracy trade-offs associated with the physically-based simulation of these phenomena. This analysis may be used to guide the selection of simulation parameters in order to achieve optimal color-accuracy and minimize runtime. We also propose a practical method to enable the predictive visualization of these phenomena within applications requiring interactive rates with minimal loss of accuracy. The effectiveness of the proposed techniques is demonstrated through simulations and image sequences depicting fading and yellowing caused by several years of exposure to light.

CCS Concepts

•**Computing methodologies** → **Physical simulation;** *Reflectance modeling;*

Keywords

natural phenomena, physically-based simulation, visualization.

1. INTRODUCTION

Images of computer generated objects typically lack signs of wear normally found in actual materials. These signs provide subtle, yet important visual cues that impart a sense of realism. Some of the most ubiquitous of these signs are associated with changes in material appearance [13] induced by exposure to light over an extended period of time (Figure 1). For instance, a painting may fade over several years of exposure to sunlight, with some colours fading more readily than others. A carpet may fade unevenly over time due to variations in light exposure depending on the location of the window and the placement of furniture. Paper and

CASA 2016, May 23 - 25, 2016, ,

ISBN 978-1-4503-4745-7/16/05…$15.00

DOI: http://dx.doi.org/10.1145/2915926.2915945

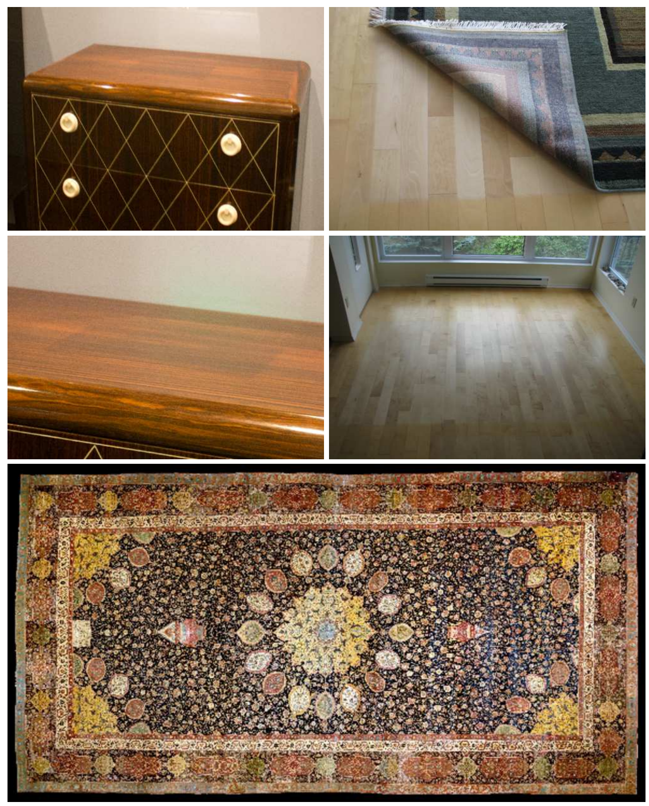

Figure 1: Photographs depicting material appearance changes induced by extended periods of light exposure. ***Top-Left, Middle-Left*****: A piece of art nouveau furniture (c. 1900, on exhibit at the Royal Ontario Museum, Toronto, Canada) whose surface has faded except where a lamp stood.** ***Top-Right, Middle-Right*****: Wood flooring darkened from light exposure except where covered by a rug.** ***Bottom*****: A carpet that has faded due to many years of light exposure (The Ardabil Carpet on exhibit at the Victoria and Albert Museum, London, United Kingdom).**

wood products turn yellow over many years of exposure to ultraviolet radiation.

Recently, the authors developed a framework for simulating the effects of light exposure over time [18] based on volumetric radiative-transfer theory. The framework employs a physicochemical approach to simulate the effect of light exposure on constituent pigments based on the amount of radiation absorbed, which is proportional to the local fluence rate. The focus of that investigation was to develop a physically-based framework to enable accurate simulations of these processes. In contexts requiring a high degree of interactivity, particularly when simulations of a large number of colourant mixtures is needed, the framework as proposed may not be sufficient to produce results in a timely manner. The goal of the present research is to provide an analysis of the influence of the key parameters of this framework on its performance characteristics, and to propose acceleration strategies for the predictive visualization of spectral changes induced by light exposure at interactive rates.

The remainder of this paper is organized as follows. In Section 2, we review related work in the computer graphics and conservation literature. In Section 3, we provide a brief outline of the light exposure framework that provides the basis for this investigation. In Section 4, we discuss the key parameters of the framework and evaluate their influence on the accuracy of the results yielded by light exposure simulations. In Section 5, we propose a method to accelerate the simulation process for large numbers of samples derived from mixtures of a relatively small set of constituent pigments. In Section 6, we outline directions for future research in this area.

2. RELATED WORK

2.1 Aging and Weathering Phenomena

There have been several works pertaining to aging and weathering phenomena. In computer graphics, Dorsey and Hanrahan [4] proposed a layered erosion and deposition model to simulate the development of metallic patinas. Dorsey *et al.* [5] simulated water flow over a surface and proposed techniques to account for the resulting changes in appearance. Kider *et al.* [17] employed a biologically based model to simulate deterioration of fruit, and Kanazawa *et al.* [16] proposed a method for rust aging simulation based on a probabilistic cellular automaton model. More recently, Guo and Pan [10] presented a framework for simulating and rendering the deposition of dust layers, and Iglesias-Guitian *et al.* [14] proposed a model for reproducing the appearance of aged skin. The reader may refer to Dorsey *et al.* [6] or Mérillou and Ghazanfarpour [21] for more detailed surveys of this body of research.

In the conservation literature, teams at the Harvard Art Museum and the MIT Media Lab collaborated to develop computational techniques for transforming measured colour changes into patterns of illumination that may be projected onto faded murals in order to restore them to their original appearance [11]. In contrast to traditional art restoration techniques, this approach preserves the original artifact, and it is completely reversible. Berns [2] and Berns *et al.* [3] proposed methods for digital restoration of paintings by using a single-constant Kubelka-Munk model to compute the intermediate appearance stages of faded artwork, given measured spectral properties of the faded and unfaded pigments. Despite these recent advancements, little attention has been paid to simulating effects induced by light exposure, such as fading and yellowing.

2.2 Acceleration Techniques

Often, simulation techniques are initially developed with accuracy and precision in mind. In such instances, considerations of performance are often secondary. Consequently, it is common in the computer graphics literature to find works aimed at extending these initial developments to enable their practical integration into standard imaging systems. For example, Preetham *et al.* [23] employed numerical techniques to allow for the practical use of a skylight model (proposed by Nishita *et al.* [22]) in realistic image synthesis applications. Similarly, the present work builds upon previously developed algorithms with the goal of enabling their use in applications requiring interactive performance.

3. FRAMEWORK

Due to its relevance for the research presented in this paper, for completeness, we briefly outline in this section the key numerical aspects of the underlying framework [18] for simulating the time-dependent effects of light exposure on spectral appearance attributes. The framework relies on volumetric radiative-transfer theory [1]. It employs a physicochemical approach to account for the effect of absorbed radiation on the absorptive properties of the medium's constituent colourants. Within this framework, a layered fading model based on Kubelka-Munk theory [20] was employed to simulate the fading and yellowing of several sample material specimens.

The domain was discretized in the vertical depth (z) and the time (t) dimensions. The solution was then computed for each dimension in turn. At a given instant in time, the light environment was evaluated throughout the medium. The absorption and scattering properties were held constant within each layer. The upward and downward radiant flux densities were evaluated at each layer boundary. These two quantities were added to compute the fluence rate at the layer boundaries. To advance to the next time step, the fluence rates were held constant over the course of the time interval, and the consequent effects on the absorptive and scattering properties of the medium were evaluated for the adjacent layers. This process was repeated for each time step in order to simulate fading over an extended period of time.

3.1 Assessing the Light Environment

To solve for the radiant flux densities $E^d(z)$ and $E^u(z)$ at a fixed time, a discretization was applied along the z-axis into N layers and the absorption and scattering were hold constant within each layer. Using these approximations, the reflectance, ρ, and transmittance, τ, of that layer could be computed using Kubelka's formulae [19] for a medium having finite depth and zero ground reflection. Since each layer was presumed to have uniform scattering and absorption properties throughout, the reflectance and transmittance of each layer was the same from below as from above. Additionally, we defined $\rho_{-1} = 0$ to be the reflectance of the infinite, non-scattering top layer and $\rho_N = \rho^*$ to be the ground reflectance.

Let E_i^d and E_i^u denote the downward and upward radiant flux densities, respectively, at the i^{th} layer boundary,

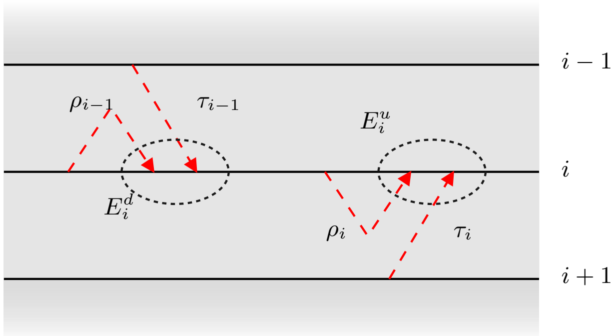

Figure 2: Diagram depicting the light paths that contributed to the upward and downward radiant flux densities, E, at the i^{th} layer interface in terms of of the radiant flux densities at the adjacent layer interfaces and in terms of the reflectances (ρ) and transmittances (τ) of the adjacent layers.

for $0 \le i \le N$. These values were expressed in terms of the reflectances and transmittances of the adjacent layers, and in terms of the radiant flux densities at the adjacent layer boundaries. Figure 2 depicts the components that contributed to the upward and downward radiant flux densities at a given layer interface. This yielded the following system of equations:

$$E_i^u = \rho_i E_i^d + \tau_i E_{i+1}^u \qquad 0 \le i < N \qquad (1)$$

$$E_i^d = \tau_{i-1} E_{i-1}^d + \rho_{i-1} E_i^u \qquad 0 < i \le N. \qquad (2)$$

The boundary conditions were $E_0^d = E_0$ and $E_N^u = \rho_N E_N^d$. This could be expressed as a system of $2(N+1)$ equations as shown in Figure 3.

The fluence rates at the layer boundaries were then given by $\vec{F} = \mathbf{E}^d + \mathbf{E}^u$. The mean fluence rate within layer i was estimated by taking the average of the fluence rates at the boundaries. The spectral fluence rate F_λ could be computed independently for each wavelength.

3.2 Updating the Absorption and Scattering Coefficients

Time stepping proceeded by solving a differential equation describing how the volume fraction, f, of a colourant evolved over time. Conservation of energy necessitates that light be absorbed in order to induce fading. The energy of a photon cannot induce a photochemical reaction and also be re-emitted as scattered light. This is known as the Grotthus-Draper law [8]. Accordingly, the response of a colourant to incoming light was determined by the amount of *absorbed* radiation. Specifically, the volume fraction was updated according to

$$f(t+\Delta t) = f(t)\exp\left(-\Delta t \int_0^\infty \beta \mu^a F_\lambda \, d\lambda\right), \qquad (3)$$

where F_λ was the spectral fluence rate at wavelength λ, μ^a was the absorption coefficient, and β was a coefficient denoting how sensitive the colourant was to absorbed radiation. The spectral fluence rate F_λ was computed for a fixed set of wavelengths using the procedure described in the previous section. The absorption coefficient μ^a was sampled at the same set of wavelengths. The result was then integrated numerically. Finally, the absorption and scattering coefficients could be updated according to

$$\mu^a(t+\Delta t) = \frac{f(t+\Delta t)}{f(t)}\mu^a(t), \qquad (4)$$

$$\mu^s(t+\Delta t) = \frac{f(t+\Delta t)}{f(t)}\mu^s(t). \qquad (5)$$

This process was performed separately for each colourant within the medium.

4. INFLUENCE OF KEY PARAMETERS

The main parameters that influence the accuracy of the results produced by the layered fading model include the number of layers and the number of time steps. We discuss the impact of these parameters below and analyse their effects on the accuracy and performance of the simulations. This analysis may be used to guide the selection of these key parameters in order to maximize accuracy of a fading simulation while minimizing the runtime cost.

4.1 Number of Layers

Within a layer, the medium is treated as fading uniformly throughout its depth. This is an approximation of actual fading behavior, where fading will be more pronounced on the exposed side of the layer than the unexposed side. The difference between the fluence rate from the top of a layer to the bottom of that layer increases with greater layer thickness or optical density. Hence, the accuracy of the simulation may be improved by using increasing the number of layers.

At each time step, the solution to the block tridiagonal system shown in Figure 3, whose size is proportional to the number of layers, N, must be found. This may be solved in $O(N)$ time [15], rather than the $O(N^3)$ time that is typically required for a general system of linear equations.

4.2 Number of Time Steps

At each time step, the fluence rate is determined for each layer. The fluence rate within each layer is presumed constant during the course of the time step. The accuracy of this approximation is primarily determined by the rate of fading during the time interval. As upper layers fade, the fluence rate increases in the layers below. Thus, the more rapidly fading progresses, the less accurate the approximation is that the fluence rate remains constant. To reduce error introduced by discretization in time, more time steps may be used.

The simulation of each time step only depends on the computation of the fluence rate and absorptive properties throughout the medium at the beginning of the time step and the length of the time interval. As there is no other dependency on prior time steps, the performance is linear with respect to the number of time steps.

4.3 Influence Assessment

As stated earlier, the key parameters affecting the behavior of the layered fading model are the number of layers and the number of time steps. The selection of values for these parameters represents a trade-off between run-time performance and minimization of discretization error. To assess the effects of these parameters, fading simulations were performed using samples consisting of random mixtures of three primary colourants: cyan, magenta, yellow.

$$
\begin{pmatrix} E_0^u \\ E_0^d \\ E_1^u \\ E_1^d \\ \vdots \\ E_{N-1}^u \\ E_{N-1}^d \\ E_N^u \\ E_N^d \end{pmatrix}
=
\begin{pmatrix}
0 & \rho_0 & \tau_0 & 0 & & & & & & \\
\rho_{-1} & 0 & 0 & 0 & & & & & & \\
0 & 0 & 0 & \rho_1 & \tau_1 & 0 & & & & \\
0 & \tau_0 & \rho_0 & 0 & 0 & 0 & & & & \\
 & & \ddots & & \ddots & & \ddots & & & \\
 & & & & 0 & 0 & 0 & \rho_{N-1} & \tau_{N-1} & 0 \\
 & & & & 0 & \tau_{N-2} & \rho_{N-2} & 0 & 0 & 0 \\
 & & & & & & 0 & 0 & 0 & \rho_N \\
 & & & & & & 0 & \tau_{N-1} & \rho_{N-1} & 0
\end{pmatrix}
\begin{pmatrix} E_0^u \\ E_0^d \\ E_1^u \\ E_1^d \\ \vdots \\ E_{N-1}^u \\ E_{N-1}^d \\ E_N^u \\ E_N^d \end{pmatrix}
+
\begin{pmatrix} 0 \\ E_0 \\ 0 \\ 0 \\ \vdots \\ 0 \\ 0 \\ 0 \\ 0 \end{pmatrix}
$$

Figure 3: The block tridiagonal system of equations, with blocks of 2×2, describing the radiant flux densities at each of the layer boundaries resulting from irradiance E_0 from above. Note that E_i^u and E_i^d represent the upward and downward radiant flux density of the i^{th} layer boundary, and that ρ_i and τ_i represent the reflectance and transmittance of the i^{th} layer.

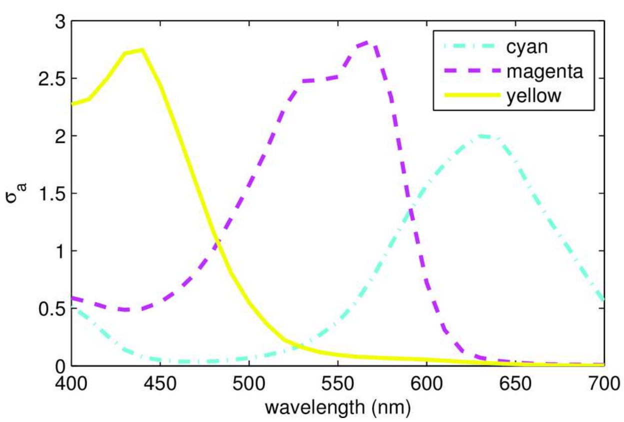

Figure 4: Optical depth associated with absorption of the three colourants (at full concentration) used in the assessment of the fading simulation parameters.

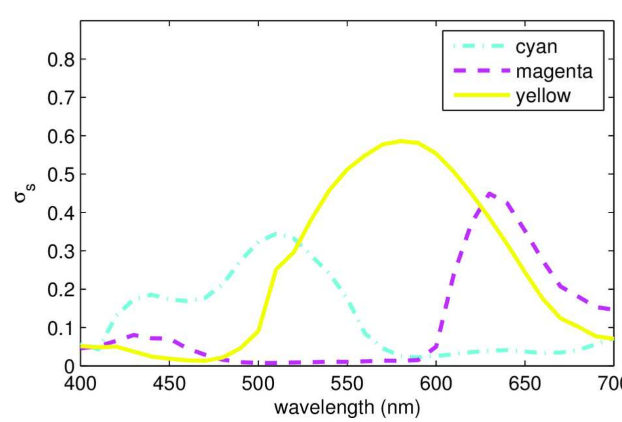

Figure 5: Optical depth associated with scattering of the three colourants (at full concentration) used in the assessment of the fading simulation parameters.

The Kubelka-Munk absorption and scattering coefficients for these colourants were derived from measurements by Yang [25] of optical depth at full concentration, which are provided in Figures 4 and 5, respectively.

Note that, in the case of absorption, the optical depth is commonly expressed as

$$\sigma_a(\lambda) = \ln\left(\frac{\Phi_i(\lambda)}{\Phi_a(\lambda)}\right), \tag{6}$$

where Φ_i and Φ_a correspond to the spectral radiant fluxes received and absorbed by the material, respectively. Similarly, in the case of scattering, the optical depth is usually expressed as

$$\sigma_s(\lambda) = \ln\left(\frac{\Phi_i(\lambda)}{\Phi_s(\lambda)}\right), \tag{7}$$

where Φ_s represents the spectral radiant flux scattered by the material. We remark that the absorption and scattering coefficients for a given sample can be obtained by dividing the corresponding optical depth quantity (σ_a and σ_s, respectively) by the sample depth (thickness) [7]. For simplicity,

	max RMS(ΔR)	Time Steps		
		5	25	125
Layers	2	0.0626	0.0352	0.0302
	4	0.0371	0.0129	0.0085
	8	0.0311	0.0071	0.0027
	16	0.0297	0.0058	0.0013
	32	0.0293	0.0055	0.0010
	64	0.0292	0.0054	0.0009
	128	0.0292	0.0054	0.0009

Table 1: Spectral difference between the results of fading simulated using varying numbers of layers and time steps and a reference simulation using 1024 layers and 625 time steps. Ten random samples were selected and fading was simulated. For each sample, the RMS ΔR was computed. The values indicated are the maximum RMS ΔR over all of the samples.

	max ΔE	Time Steps		
		5	25	125
Layers	2	6.2203	3.8875	3.4764
	4	3.3564	1.2955	0.9543
	8	2.7686	0.6476	0.2844
	16	2.6603	0.5102	0.1225
	32	2.6333	0.4882	0.0872
	64	2.6265	0.4827	0.0811
	128	2.6248	0.4813	0.0798

Table 2: Color difference between the results of fading simulated using varying numbers of layers and time steps and a reference simulation using 1024 layers and 625 time steps. The values indicated are the maximum ΔE over ten randomly selected samples.

in our simulations described in this paper, we consider the samples' thickness equal to 1 arbitrary unit of length.

The number of layers and time steps were varied and the results compared for colour and spectral accuracy to a reference simulation using 1024 layers and 625 time steps.

To assess spectral accuracy, we computed the spectral difference between the results of fading simulated using varying numbers of layers and time steps and a reference simulation using 1024 layers and 625 time steps. More specifically, ten random samples were selected and fading was simulated. The reflectance of each selected sample was then compared to the reflectance given by the corresponding reference simulation. This comparison involved the computation of the corresponding root-mean-square (RMS) difference [9] between these two reflectance curves. The maximum RMS difference across all samples is given in Table 1 for various combinations of the key parameters.

To assess colour accuracy, the reflectance curves generated by the simulation are transformed to the CIE Lab colour space [12, 24]. Table 2 shows the maximum ΔE, the Euclidean distance in the CIE Lab colour space, between the trial simulation and the corresponding reference simulation. This distance is a measure of the perceptual difference between two colours, with $\Delta E = 1$ representing a *just noticeable difference*.

Table 3 shows the average run-time (across all samples) required to simulate fading. The simulations were performed using a single core on a machine with two 2.8 GHz quad-core Xeon E5462 processors and 16 GB of RAM.

	time (s)	Time Steps		
		5	25	125
Layers	2	0.6	2.9	14.0
	4	0.7	3.2	15.4
	8	0.8	3.6	17.6
	16	1.0	4.4	21.5
	32	1.5	6.3	30.7
	64	3.5	15.8	76.6
	128	8.6	36.8	179.0

Table 3: Time (averaged across all samples) required to simulate fading using the varying numbers of layers and time steps.

Figure 6 depicts visualizations of two sequences of photographs demonstrating fading over an extended period of time. These sequences employ the same settings as for the reference simulations, *i.e.*, 1024 layers and 625 time steps. Figure 8 provides a visual depiction of the effect of using varying number of layers and time steps.

5. SELECTIVE INTERPOLATION

Besides reducing the number of layers and time steps, guided by the analysis discussed in the previous section, we may also use interpolation techniques to reduce the cost of simulating fading for a large number of samples consisting of varying mixtures of a small set of pigments.

A typical high definition image consists of over two million pixels and may contain hundreds of thousands of unique colours. As such, it is prohibitively expensive to run a simulation for each colour in the image. For typical fading scenarios, there are only a few pigments involved. The colours to be faded consist of varying mixtures of these pigments. For mixtures of n pigments, we obtain a corresponding n-dimensional space arising out of the varying concentrations of each pigment. This space may be divided into a grid, and fading simulated only at grid points. For example, considering the n axes corresponding to the n pigments, and sampling at m points along each axis, this would result in m^n grid points.

To determine the reflectance of a faded sample consisting of a different mixture of these pigments, we interpolate between grid points. By dividing a three-dimensional colour space (such as CMY [24]) into a coarse grid, we only need to simulate fading for a comparatively small number of pigment combinations. In our simulations, we found that the use of a $6 \times 6 \times 6$ grid (216 grid points) yielded results comparable to the reference simulation. For different scenarios, a coarser or finer grid may be employed. Using this selective interpolation approach, fading results may then be computed at interactive rates.

Figure 7 shows a comparison of a photograph with fading applied with and without interpolation as described above. The simulation without selective interpolation required 218.3 hours to complete. In contrast, the $6 \times 6 \times 6$ grid took 6.3 hours to generate, after which multiple images may be generated instantaneously. Figure 9 shows visualizations of a scene subjected to light exposure over the course of several years. The dresser has faded except where the lamp stood. The rug has faded, and the wood floor has turned yellow except where the rug was placed. These renderings illustrate the use of this framework in realistic image synthesis

Figure 6: Reference visualizations of two photographs faded according to the framework using 1024 layers and 625 time steps. The leftmost images depict the initial (unfaded) state of the photographs. The remaining images depict the photographs faded over progressively longer time periods.

applications. The rug and the dresser were faded by approximating the initial state (prior to light exposure) as a combination of the primary pigments depicted in Figures 4–5 and using the same techniques applied to the photographs in Figures 6–7. The fading of the wood floor was simulated using absorption data for lignin and orthoquinones provided elsewhere [18].

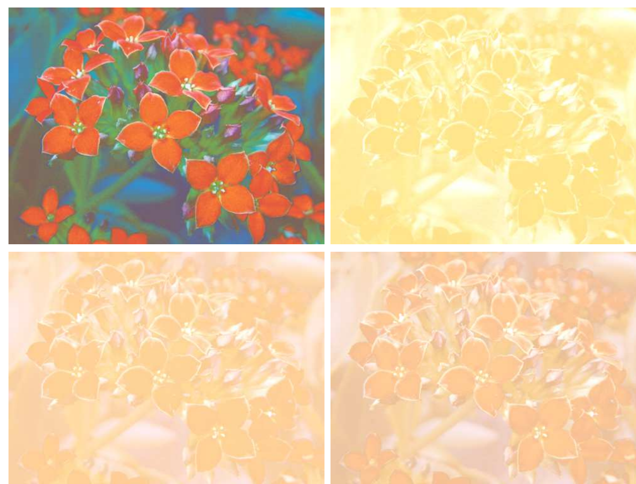

Figure 8: Photograph faded using varying numbers of layers and time steps. *Top-Left:* Initial (unfaded) state of the photograph. *Top-Right:* Faded using two layers, five time steps. *Bottom-Left:* Faded using 128 layers, 125 time steps. *Bottom-Right:* Reference rendering, faded using 1024 layers, 625 time steps.

6. CONCLUSION AND FUTURE WORK

Computer generated scenes typically lack the signs of wear that provide important visual cues and increase the sense of realism. Light-exposure driven phenomena, such as fading and yellowing, are arguably among the most important of these signs for indoor scenes. In this work, we have examined the effect of key parameters on the performance characteristics of a recently proposed framework for simulating light-exposure effects. We have also proposed techniques for allowing the framework to be employed at interactive rates with minimal loss of accuracy.

In the future, we intend to modify the underlying fading framework to allow for dynamic, non-uniform layer thicknesses. By using thinner layers where the fluence rate changes more sharply, a higher degree of accuracy may be achieved with fewer layers. Allowing these layer thicknesses to vary from one time-step to another will allow the system to adapt as the colourant distribution evolves. We also intend to investigate the use of this framework as the basis for inversion procedures for assisting in the restoration of faded works of art.

7. REFERENCES

[1] J. Arvo. Transfer equations in global illumination. In *SIGGRAPH '93 Course Notes*, volume 42, Aug. 1993.

[2] R. Berns. Rejuvenating the appearance of cultural heritage using color and imaging science techniques. In *Proceedings of the 10th Congress of the International Colour Association*, pages 369–374, 2005.

[3] R. Berns, S. Byrns, F. Casadio, I. Fiedler, C. Gallagher, F. Imai, A. Newman, M. Rosen, and L. Taplin. Rejuvenating the appearance of Seurat's *a sunday on la grande jatte – 1884* using color and imaging science techniques - a simulation. In *Proceedings of the 10th Congress of the International Colour Association*, pages 1669–1672, 2005.

[4] J. Dorsey and P. Hanrahan. Modeling and rendering of metallic patinas. In *Computer Graphics Proceedings, Annual Conference Series*, pages 387–396, 1996.

[5] J. Dorsey, H. Pedersen, and P. Hanrahan. Flow and changes in appearance. In *Computer Graphics Proceedings, Annual Conference Series*, pages 411–420, 1996.

[6] J. Dorsey, H. Rushmeier, and F. Sillion. *Digital Modeling of Material Appearance*. Morgan Kaufmann/Elsevier, 2008.

[7] W. Egan and T. Hilgeman. *Optical Properties of Inhomogeneous Materials: Applications to Geology, Astronomy, Chemistry, and Engineering*. Academic Press, New York, NY, USA, 1979.

Figure 7: Visualization of a photograph fading with and without selective interpolation. ***Left:*** **Original photograph.** ***Center:*** **Reference rendering using** 1024 **layers and** 625 **time steps.** ***Right:*** **Visualization using interpolation over a** $6 \times 6 \times 6$ **grid.**

[8] C. Giles and R. McKay. The lightfastness of dyes: A review. *Textile Research Journal*, 33(7):528–575, July 1963.

[9] A. Glassner. *Principles of Digital Image Synthesis*, volume 2. Morgan Kaufmann Publishers, Inc., San Francisco, CA, 1995.

[10] J. Guo and J. Pan. Real-time simulating and rendering of layered dust. *The Visual Computer*, 30(6):797–807, June 2014.

[11] J. Hecht. Light repairs art: optical overlays restore faded masterworks. *Optics & Photonics News*, 26(4):40–47, Apr. 2015.

[12] R. Hunt. *Measuring Color*. Ellis Horwood, New York, NY, USA, second edition, 1991.

[13] R. Hunter and R. Harold. *The Measurement of Appearance*. John Wiley & Sons, New York, NY, USA, second edition, 1987.

[14] J. Iglesias-Guitian, C. Aliaga, A. Jarabo, and D. Gutierrez. A biophysically-based model of the optical properties of skin aging. *Computer Graphics Forum*, 34(2):45–55, 2015.

[15] E. Isaacson and H. Keller. *Analysis of Numerical Methods*. Dover Publications, Inc., Mineola, NY, 1994.

[16] K. Kanazawa, R. Tanabe, T. Moriya, and T. Takahashi. Rust aging simulation considering object's geometries. In *SIGGRAPH 2015 Posters*, Aug. 2015. Article 54.

[17] J. Kider, S. Raja, and N. Badler. Fruit senescence and decay simulation. *Computer Graphics Forum*, 30(2):257–266, Apr. 2011. Proceedings of EUROGRAPHICS 2011.

[18] B. Kimmel, G. Baranoski, T. Chen, D. Yim, and E. Miranda. Spectral appearance changes induced by light exposure. *ACM Transactions on Graphics*, 32(1):10:1–10:13, Jan. 2013.

[19] P. Kubelka. New contributions to the optics of intensly light-scattering materials. Part I. *Journal of the Optical Society of America*, 38(5):448–457, May 1948.

[20] P. Kubelka and F. Munk. Ein beitrag zur optik der farbanstriche (An article on optics of paint layers). *Zeitschrift für Technische Physik*, 12:593–601, Aug. 1931.

[21] S. Mérillou and D. Ghazanfarpour. A survey of aging and weathering phenomena in computer graphics. *Computers & Graphics*, 32(2):159–174, Apr. 2008.

[22] T. Nishita, T. Sirai, K. Tadamura, and E. Nakamae. Display method of the sky color taking into account multiple scattering. In *Pacific Graphics '96*, pages 117–132, 1996.

[23] A. Preetham, P. Shirley, and B. Smits. A practical analytic model for daylight. In *Computer Graphics (SIGGRAPH Proceedings)*, pages 91–100, Aug. 1999.

[24] M. Stone. *A Field Guide to Digital Color*. A K Peters, Natick, MA, 2003.

[25] L. Yang. Modelling ink-jet printing: Does the Kubelka-Munk theory apply? In *International Conference on Digital Printing Technologies*, volume 18, pages 482–485. Society for Imaging Science and Technology, Sept. 2002.

Figure 9: Sequence of images depicting a scene in which a dresser, rug, and wood floor are subjected to light exposure over the course of several years. *Top Left:* Prior to light exposure. *Top Right:* After several years of exposure, the rug and dresser have faded and the wood floor has yellowed. *Bottom:* The rug and lamp have been removed, revealing the effects of light exposure on the dresser and on the wood floor.